Excited State Tautomerization of 7-Azaindole in a 1:1 Complex with δ-Valerolactam: A Comparative Study with the Homodimer

ARTICLE *in* THE JOURNAL OF PHYSICAL CHEMISTRY A · SEPTEMBER 2012

Impact Factor: 2.69 · DOI: 10.1021/jp306959w · Source: PubMed

3 AUTHORS:

Moitrayee Mukherjee
Indian Association for the Cultivation of Science
18 PUBLICATIONS **60** CITATIONS
SEE PROFILE

Shreetama Karmakar
Indian Association for the Cultivation of Science
6 PUBLICATIONS **10** CITATIONS
SEE PROFILE

Tapas Chakraborty
Indian Association for the Cultivation of Science
107 PUBLICATIONS **838** CITATIONS
SEE PROFILE

THE JOURNAL OF PHYSICAL CHEMISTRY A

Article

pubs.acs.org/JPCA

Excited State Tautomerization of 7-Azaindole in a 1:1 Complex with δ-Valerolactam: A Comparative Study with the Homodimer

Moitrayee Mukherjee, Shreetama Karmakar, and Tapas Chakraborty*

Department of Physical Chemistry, Indian Association for the Cultivation of Science, Jadavpur, Calcutta 700032, India

ABSTRACT: A comparative analysis for relative stability between normal and tautomeric forms in the excited electronic states of 7-azaindole···δ-valerolactam 1:1 complex and 7-azaindole homodimer has been presented. The tautomeric configuration of the complex is estimated to be ∼6 kcal/mol more stable than normal form, and the same for homodimer appears to be ∼10 kcal/mol. Consistent with these estimates both the complex and homodimer undergo facile double proton transfer tautomerization upon UV excitation in hydrocarbon solutions (Chou; et al. *J. Am. Chem. Soc.* **1995**, *117*, 7259). However, we notice that such similarity in photophysical behavior of the two hydrogen-bonded systems is lost completely in a cold supersonic jet expansion. The jet-cooled homodimer emits only the tautomer fluorescence in the visible spectral region, but the complex emits exclusively from the locally excited state in ultraviolet. We have interpreted this contrast by arguing that the effective barrier for excited state double proton exchange tautomerization of the complex is larger compared to that of the homodimer, and the difference originates because of asymmetric nature of the two hydrogen bonds of the complex.

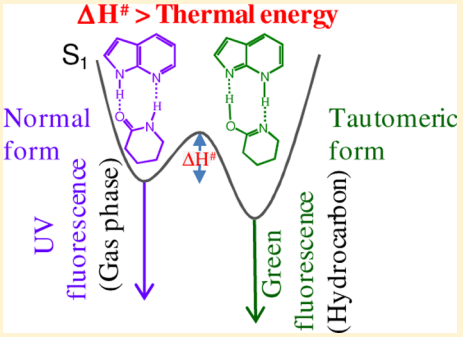

INTRODUCTION

Light-induced tautomerization of 7-azaindole (7AI) in doubly hydrogen bonded dimeric complexes has received much attention over the past several decades as a paradigm system to understand the microsolvation and double proton transfer photophysics.[1−19] These complexes have also been considered as mimics of the nucleobase pairs, whose tautomeric changes could cause mismatch in interstrand pairing leading to errors in DNA replication.[20,21] In the 7AI-homodimer ($7AI_2$), the tautomerization is depicted as a simultaneous exchange of two N−H protons along the two identical intermolecular N−H···N hydrogen bonds (Figure 1), which does not occur in the ground state, but occurs upon absorption of a UV photon. The primary driving force of the process is the enhanced acid−base character of the molecule in the excited state, which originates due to intramolecular charge displacement from the pyrrolic and to pyridinic rings.[9] Such charge reorganization facilitates release of the pyrrolic proton of the excited moiety to the acceptor, and abstraction of a proton from the donor to the pyridine site. Much effort has been devoted to resolve whether this exchange of the two protons in the homodimer takes place sequentially or in a concerted manner.[12] An important issue in this regard is the role played by the medium in assisting the proton transfers. In nonpolar hydrocarbon liquids, the excited state tautomerization of the homodimer has been found to be extremely efficient, and the proton exchange takes place on an ultrafast time scale.[1,2,10,11] The process also occurs very efficiently in the cold environment of a supersonic jet expansion.[3,4,8] In fact, Sakota et al. have shown that the tautomerization under the latter condition occurs exclusively even from the lowest level in S_1 (0°).[8] Thus, no medium assistance is required for occurrence of the excited state proton exchange in the $7AI_2$. However, we show here that the same is not true for a mixed dimer, i.e., 1:1 type complex between 7AI and a six-member cyclic amide, δ-valerolactam (δVL), although the structure and binding energy of this complex are very similar to those of $7AI_2$ and from energetic viewpoint the excited state double proton transfer (ESDPT) tautomerization of the complex is a favored process.

Two vital energetic parameters concerning the ESDPT dynamics are the energy barrier (ΔE^{*}_{N-T}), and energy gap between the normal and tautomeric forms ($\Delta E^{S_1}_{N-T}$). In the case of $7AI_2$, the conversion barrier has always been considered to be low (∼1 kcal/mol),[1,3,5] but its existence is revealed by observing distinct isotope effect on tautomeric conversion yield and rate.[8] Concerning $\Delta E^{S_1}_{N-T}$, one can make a reliable estimate of this parameter from the measured values of electronic transition energies ($\Delta E^{S_1}_{S_0}$) under an isolated condition of the normal and tautomeric forms and the calculated energy difference of the two tautomeric forms in the ground state ($\Delta E^{S_0}_{N-T}$), as discussed in the Energetics section below. In the present paper we have analyzed a remarkable medium effect on ESDPT dynamics of 7AI···δVL complex revealed in the measurements described in the following sections in terms of these two energetic parameters. The photophysics of this complex in a hydrocarbon solution was studied earlier by Chou et al., which shows efficient tautomerization at room temperature.[22] The hydrogen-bonded interface of this complex (Figure 1) resembles those of adenine−thymine and

Received: July 13, 2012
Revised: September 15, 2012
Published: September 17, 2012

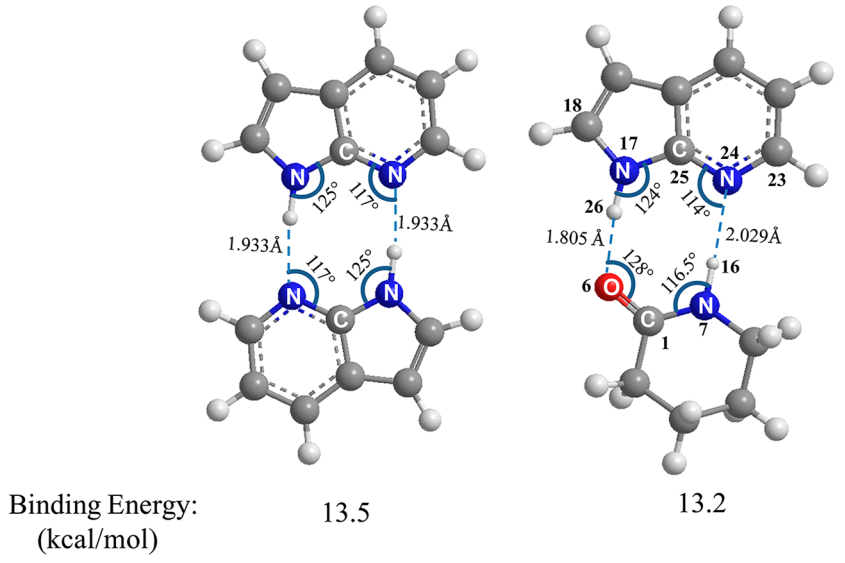

Figure 1. Optimized geometries of $7AI_2$ and 1:1 complex between 7AI and δVL calculated at DFT/B3LYP/6-311++G** level. Some relevant geometrical parameters of the hydrogen bonded interface of the two systems are also shown. The binding energies are shown after BSSE correction.

adenine−uracil base pairs, and thus it is a more realistic mimic of the base pairs compared to that of the 7AI homodimer. The ESDPT tautomerization of 7AI in the complex leads to simultaneous tautomerization of the δVL moiety from the lactam to the lactim form. Thus, the ESDPT event of this complex is characteristically very different in comparison to the same in complexes with alcohols,[13,14] water,[15−17] and carboxylic acids.[18,19] In all these cases the complexing species act as catalysts and remain unchanged. Therefore, understanding of the detailed photophysics of the present complex could be beneficial to understand the tautomeric changes in base pairs. In the present study we have attempted to probe the intrinsic photophysical behavior of the complex by measuring the laser-induced fluorescence spectra (LIF) in a supersonic jet expansion and comparing the observations with those in a hydrocarbon solution at room temperature. An energetic analysis is also presented to assess whether the ESDPT tautomerization is an intrinsic attribute of the complex, i.e., can take place under a supersonic jet expansion condition, or is induced by the medium.

EXPERIMENTAL DETAILS

The compounds, 7AI and δVL, were procured from Sigma Aldrich, and they were purified further by vacuum sublimation. In our experimental arrangement the compounds were vaporized in two separate compartments, by heating at temperatures 60−80 °C, and the vapors were mixed with the carrier gas helium at a pressure of 1−2 atm. The final gas mixture was expanded into vacuum through a pulsed nozzle (General Valve, series-9) of orifice diameter 0.5 mm for supersonic jet expansion, where the complexes were formed due to intermolecular collisions, and cooled further along the jet. At about 10 mm downstream of the nozzle orifice, the complexes were excited by the frequency-doubled output of a tunable dye laser (Continuum, Model: ND6000), which was pumped by the second harmonic (λ = 532 nm) of a Nd:YAG laser (Litron, Model: TRS 10). The line width of the tunable UV laser is <0.1 cm^{-1} and per pulse energy ~500 μJ. The fluorescence was collected from the intersection point of the laser and jet in a direction perpendicular to both beams. The fluorescence excitation (FE) spectra were measured by detecting total as well as different segments of fluorescence using an IP28 photomultiplier tube. The UV fluorescence was selected by using a combination of UV32 and U330 glass filters in front of the PMT tube, and the effective wavelength transmission of the filter combination was 320−400 nm (shown below). For visible fluorescence detection, an optical glass filter that transmits wavelengths >400 nm was used (UV/IR cutoff filter, Edmund Optics). The output signal of the PMT was processed using a boxcar averager (Stanford Research Corp., Model: SR250). The averaged output of the boxcar was stored in a computer using a home-built data acquisition system and the spectra were plotted using the origin software package.[23]

COMPUTATIONAL DETAILS

The geometries and binding energies of the 7AI···δVL complex and homodimer in the ground electronic state were calculated by DFT/B3LYP/6-311++G** theoretical method. The basis set superposition error (BSSE) corrections in the binding energies of the complexes were calculated by the counterpoise (CP) method of Boys and Bernardi,[24] as implemented in the Gaussian-03 program package.[25] The vertical electronic transition energies for the normal and tautomeric forms of the complex and homodimer were calculated by TDDFT method using the same basis set. The excited state (S_1) geometry and vibrational normal-mode frequencies of the complexes were calculated by the CIS/6-31G* method, and the corresponding values in the ground electronic state (S_0) were calculated at the HF/6-31G* level. The frequencies in the S_0 state of the complexes were calculated also using DFT/B3LYP/6-311++G** method.

RESULTS AND DISCUSSION

Energetics of the Normal and Tautomeric Forms of 7AI Complexes. The relative energies in the ground and first excited electronic states of the normal and tautomeric forms of the $7AI_2$ and 7AI···δVL complex are shown in Figure 2. The $S_1 \leftarrow S_0$ electronic transition energies for the normal forms of both the species are known accurately from the LIF excitation

dx.doi.org/10.1021/jp306959w | J. Phys. Chem. A 2012, 116, 9888−9896

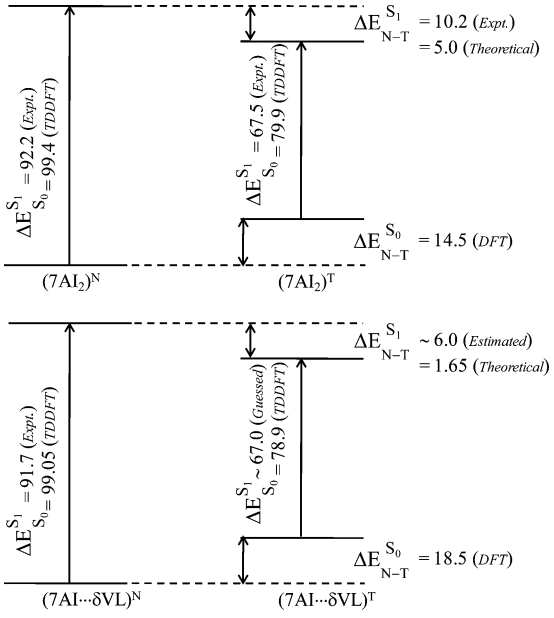

Figure 2. Schematics for the energy levels in the ground and first excited electronic states of the $7AI_2$ and 7AI···δVL complex in the two tautomeric forms. All electronic structure calculations (DFT and TDDFT) were carried out using B3LYP functional and 6-311++G** basis set.

spectra measured under the supersonic jet expansion (shown below). Interestingly, these values are found to be nearly same. This is consistent with the suggestion of a number of studies that exciton interaction of the homodimer is very small, which implies that the electronic excitation would be localized practically only on one of the moieties.[7,12] In the ground state the tautomeric forms are unstable, but their energies have been calculated. At the B3LYP/6-311++G** level the tautomeric form of the homodimer is predicted 14.5 kcal/mol higher in energy compared to the normal form and the corresponding energy difference for the complex is ∼18.5 kcal/mol.

The $S_1 \leftarrow S_0$ energy gap of the tautomeric form of the complex is also expected to be similar to that of the homodimer, because it has been found that the fluorescence spectra of both the species in hydrocarbon solution look identical (see below). Using the REMPI method the S_1-S_0 energy gap of this form of homodimer (67.5 kcal/mol) has been measured recently by Ishikawa et al.[26] For the complex, on the basis of the above mention arguments, we guess it to be similar (∼67 kcal/mol) to that of the homodimer. Combining these data, one estimates from the energy level scheme shown in Figure 2 that the tautomeric state in S_1 of the homodimer is 10.2 kcal/mol lower compared to its normal form, and this energy difference for the 7AI···δVL complex is ∼6.0 kcal/mol. Thus, from an energetic viewpoint, the ESDPT tautomerization of the complex under an isolated condition is expected to be an exothermic process. In Table 1, a comparison of the calculated values of this energy gap ($\Delta E^{S_1}_{N-T}$) for homodimer, reported by various authors, is shown.[27−33] Although the tautomeric form is always predicted to be lower in energy with respect to the normal form, the energy gap values are quite diverse. For the 7AI···δVL complex, the prediction of the electronic structure calculation performed at TDDFT/6-311++G** level also is consistent with the above-mentioned estimate (Figure 2). Therefore, the energy gap parameter ($\Delta E^{S_1}_{N-T}$) indicates that

Table 1. Theoretically Predicted Values for the Energy Gap between Normal and Tautomeric Forms of $7AI_2$ in the First Excited State ($\Delta E^{S_1}_{N-T}$) Reported to Date[a]

level of calculation (ref no.)	$\Delta E^{S_1}_{N-T}$ (kcal/mol)
LC- TDDFT/Sapporo-DZP (ref 27)	7.0
CASPT2/Sapporo-DZP (ref 27)	16.4
CASSCF/(10s5p1d)/[3s2p1d] (ref 28)	17.93
MRMP/(10s5p1d)/[3s2p1d] (ref 28)	5.30
CASSCF/6-31G** [with single point cal in CASPT2 level] (ref 29)	6.37 (5.91)[b]
TDDFT/6-31G** (ref 30)	5.3
CIS/6-31G* (ref 31)	4.18
CIS/6-31G** [with DFT optimized ground state geometry] (ref 32)	3.0
CIS/4-31G (ref 33)	2.69
TDDFT/6-311++G** (present study)	5.0

[a]The value predicted by TDDFT method of the present study is also shown. [b]Considering C_{2h} symmetry of the normal dimer.

ESDPT tautomerization of the complex should occur under an isolated condition. However, we show below that the conversion depends sensitively on medium, and particularly on its thermal condition.

Photophysics of 7AI···δVL in a Hydrocarbon Solution. The complex is easily formed at room temperature upon dissolving the two compounds (7AI and δVL) in a nonpolar aprotic solvent. In the present study, methylcyclohexane (MCH) was used as solvent, and a series of mixed solutions were prepared where in each the effective concentration of 7AI was 10^{-5} M but the concentration of δVL was varied in the range of 1.56×10^{-4} to 5×10^{-3} M. The absorption spectra corresponding to these solutions are shown in Figure 3. Trace 1 of the figure indicates that at such a low concentration of 7AI, the molecules exist predominantly in monomeric form (in

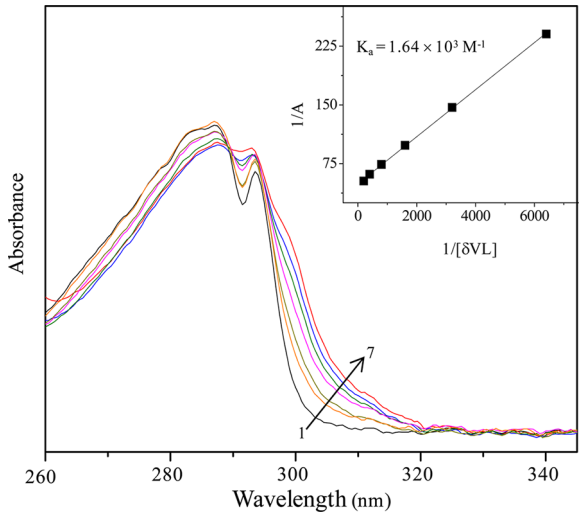

Figure 3. Complex formation effect on the longest wavelength segment of $S_1 \leftarrow S_0$ electronic absorption band of 7AI in MCH at room temperature. The concentration of 7AI in each solution is 10^{-5} M, and δVL concentration is varied in the range of 1.56×10^{-4} to 5×10^{-3} M. The black arrow across the traces indicates the increasing concentration of δVL in mixed solutions of fixed concentration of 7AI. A linear Benesi−Hildebrand plot (inset) corresponding to changes in absorption intensity at 310 nm of the complex ensures that only 1:1 complex has been formed preferentially.

dx.doi.org/10.1021/jp306959w | J. Phys. Chem. A 2012, 116, 9888−9896

absence of δVL), and the origin band for $S_1 \leftarrow S_0$ transition appears at 293 nm. With increasing concentrations of δVL in the mixed solutions due to complex formation between 7AI and δVL, new unresolved features develop in the wavelength range longer than 300 nm. A Benesi–Hildebrand analysis of intensity increase at 310 nm, shown in the inset yields a linear plot, which indicates that the complex produced in the mixed solution is predominantly 1:1 type.

The complex formation effects on fluorescence emission and excitation spectra under this condition are shown in Figure 4.

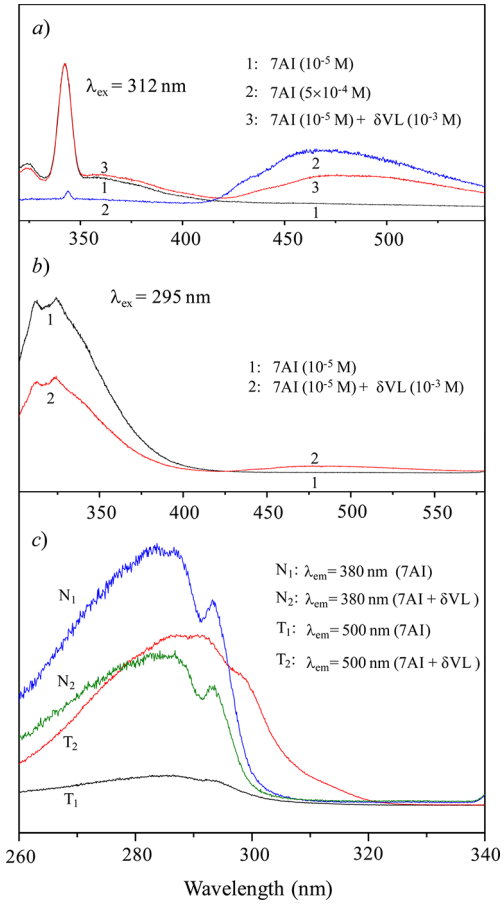

Figure 4. Fluorescence spectrum of the 7AI···δVL complex in MCH solution at room temperature for excitations at wavelengths (λ_{ex}) 312 nm (part a) and 295 nm (part b). The spectra recorded by exciting at these two wavelengths for pure 7AI solution of concentration 10^{-5} M are depicted as trace 1 in each part. Trace 2 in part a depicts the fluorescence spectrum of the homodimer in 5×10^{-4} M solution for excitation at 312 nm. The sharp features in the UV region in all spectra are the Raman bands of the solvent. Fluorescence excitation spectra of the same set of solutions for probing at wavelengths (λ_{em}) 380 and 500 nm are shown in part c.

Part a of the figure shows three emission spectra recorded by exciting the solutions at 312 nm, where only the complex or $7AI_2$ can absorb. When the dilute solution of 7AI (10^{-5} M) is excited in the absence of δVL (trace 1), the tautomer fluorescence at 500 nm is practically absent because the homodimer population at such a low concentration of 7AI is very small, but a significant extent of this emission is developed when the concentration of 7AI is high (5×10^{-4} M) (trace 2). The sharp features in the UV region in the spectra are due to Raman bands of the solvent. In the presence of δVL (10^{-3} M) in a 10^{-5} M solution of 7AI, the tautomer fluorescence that is similar to that of the homodimer shows a large enhancement (trace 3), and the behavior is the same as reported by Chou et al.[22] However, no local fluorescence in UV develops, and this absence indicates that δVL assisted tautomerization of 7AI is very efficient; i.e., the tautomerization rate is faster than the normal decay rate of the excited complex through spontaneous emission.

In part b, a comparison between two emission spectra for excitation at wavelength 295 nm is shown. This wavelength is near the $S_1 \leftarrow S_0$ electronic origin transition of the 7AI monomer, and here both $7AI_2$ and the 7AI···δVL complex also have significant absorptions. In the absence of δVL, the UV fluorescence of the 7AI monomer appears predominantly (trace 1) and the tautomer fluorescence is very weak. In the presence of δVL, the normal fluorescence is lowered with enhancement of tautomer fluorescence (trace 2).

The FE spectra corresponding to detections of tautomer fluorescence at 500 nm, and fluorescence from the locally excited state in UV at 380 nm for the same two solutions, are shown in part c of the figure. Trace T_1 indicates that a little of homodimer is still present in the solution even at such a low concentration (10^{-5} M), because the fluorescence at 500 nm can be emitted under this condition only by $7AI_2$. The longer wavelength features (>300 nm) of the dimer are not discernible in the spectrum because of overall weak intensity. In the presence of δVL, the tautomer fluorescence shows a large enhancement, and the trace T_2 shows the basic features of the excitation spectrum of the complex. This spectrum shows that the longest wavelength absorption band of the complex appears near 310 nm, and other features at shorter wavelengths are nearly similar to those of the homodimer. On the other hand, the FE spectrum recorded for detection at 380 nm of the same mixed solution (trace N_2) yields basically the FE spectrum of 7AI monomer, because the same spectrum (trace N_1) is observed with larger intensity if δVL is not added to the solution. This confirms that the complex does not emit local fluorescence, and the tautomeric conversion is as efficient as that of the homodimer. Therefore, the photophysical behavior of the complex discussed here is consistent with the energetic analysis presented before (Energetics section).

Photophysics of 7AI···δVL in a Supersonic Jet Expansion. Our primary objectives for the measurements described here are to study the intrinsic photophysical behavior of the complex and to compare the observations with the behavior of homodimer under similar experimental conditions. We hope such comparative analysis would reveal more vividly the effects arising due to asymmetry of the two hydrogen bonds on the ESDPT photophysics of the complex. The measurement would also reveal the influence of thermal equilibrium on tautomerization dynamics in an inert liquid (described above), because the latter cannot have any specific interaction with either $7AI_2$ or the 7AI···δVL complex. The LIF excitation spectra recorded under such conditions for detection of different segments of fluorescence are presented in Figure 5. The top panel shows the spectrum recorded for detection of total fluorescence, i.e., when no optical glass filter was used in front of the PMT. Here the most intense band at 32 054 cm^{-1} is assigned to the $S_1 \leftarrow S_0$ origin transition (0_0^0) of the 1:1 complex. A number of prominent low-frequency vibronic features developed on the 0_0^0 band, and these are due to excitation of the fundamentals, overtones, and combinations of different intermolecular vibrational modes of the complex in

dx.doi.org/10.1021/jp306959w | J. Phys. Chem. A 2012, 116, 9888–9896

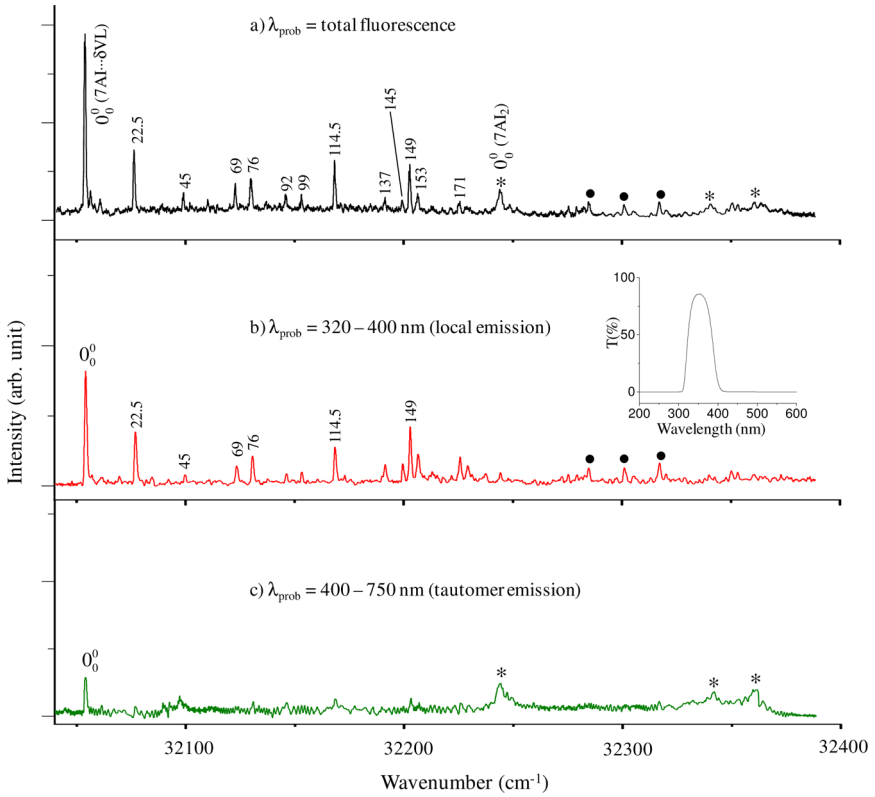

Figure 5. Fluorescence excitation spectra for $S_1 \leftarrow S_0$ excitation of 7AI···δVL complex in a supersonic jet expansion for detection of (a) total fluorescence, (b) UV fluorescence in the spectral range of 320–400 nm, and (c) visible tail of fluorescence of wavelengths longer than 400 nm. The backing pressure of the carrier gas helium is ∼1 atm. The bands denoted by asterisks (top panel) and dots belong to $7AI_2$ and 2:1 7AI-water complex, respectively. The vibronic band positions relative to the origin band (0_0^0) are labeled in panels a and b using respective frequencies (in cm^{-1}). The inset of panel b shows the transmission curve of the filter combinations used to record the UV fluorescence.

Table 2. Assignments of the Vibronic Bands in the FE Spectrum (Figure 5) of the Jet-Cooled 7AI···δVL Complex[a]

observed frequency (cm^{-1}) relative to 0_0^0 origin band[b]	calculated frequencies in S_1 (CIS/6-31G*) (cm^{-1})	mode characteristics	calculated frequencies in S_0 at HF/6-31G* level (cm^{-1})	calculated frequencies in S_0 (cm^{-1}) at DFT/6-311++G** level (cm^{-1})	assignments suggested
22.5	23 (Q_1)	out-of-plane butterfly motion	20	25	$(Q_1)_0^1$
45	42 (Q_2)	out-of-plane twisting	39	43	$(Q_2)_0^1/(Q_1)_0^2$
69	69 (Q_3)	in-plane rocking	60	70	$(Q_3)_0^1$
76	75 (Q_4)	out-of-plane rocking	72	77	$(Q_4)_0^1$
92					$(Q_1)_0^1 + (Q_3)_0^1$
99					$(Q_1)_0^1 + (Q_4)_0^1$
114.5	94 (Q_5)	in-plane sliding	84	92	$(Q_5)_0^1$
137					$(Q_1)_0^1 + (Q_6)_0^1$
145					$(Q_3)_0^1 + (Q_4)_0^1$
149	131 (Q_6)	in-plane intermolecular stretching	117	129	$(Q_6)_0^1$
153					$(Q_4)_0^2$
171					$(Q_1)_0^1 + (Q_8)_0^1$

[a]The modes labeled Q_1 to Q_6 are the six intermolecular vibrations of the complex. [b]$S_1 \leftarrow S_0$ electronic origin band of the complex is at 32 054 cm^{-1}.

the first excited state. Our suggested assignments for these bands are presented in Table 2 and discussed in detail in the Vibrational Analysis section.

The 0_0^0 origin and other low-frequency vibronic bands in $S_1 \leftarrow S_0$ absorption system of $7AI_2$ are also visible in the spectrum, and those are labeled by asterisks. The partial pressure of 7AI in the expansion gas mixture being smaller compared to that of δVL, the homodimer formation probability is lower compared to that of the 7AI···δVL complex, and thus the bands of the former appear much weaker compared to the latter, assuming that the Franck–Condon factors of the vibronic bands of the two complexes are similar. It is seen that the spectral shift of 7AI chromophore due to complexation with δVL (2571 cm^{-1}) is comparable to that in the homodimer (2381 cm^{-1}).[3,4] Such similarity in spectral shifts ensures that the complex (7AI···δVL) formed under the supersonic jet expansion adopts

dx.doi.org/10.1021/jp306959w | J. Phys. Chem. A 2012, 116, 9888–9896

a planar doubly hydrogen bonded cyclic geometry similar to that of the homodimer. A slightly larger shift for the complex is an indication for formation of N−H···O═C hydrogen bond, which is likely to be stronger than the N−H···N hydrogen bonds of the homodimer. To eliminate the possibility that some of the weaker features in this region could be due to higher sized complexes, we have measured the FE spectra by changing the backing pressure of the carrier helium gas and partial pressure of δVL in the gas mixture (by increasing the temperature of the cell containing this species), but no distinct indication for relative enhancement in intensity of any of the bands was found. Thus we infer that only a 1:1 complex is easily and preferentially formed, and this could be due to the fact that the doubly hydrogen bonded cyclic geometry gains stability due to cooperative interaction between two hydrogen bonds.

The middle and bottom panels show the FE spectra recorded by probing UV and visible segments of fluorescence, respectively. It is seen that almost all the bands in the middle trace appear with same relative intensity as they are in the top panel, but they are very weak in the bottom trace. This indicates that the complex emits predominantly in ultraviolet and fraction of fluorescence emitted in the visible region is extremely small. On the other hand, the homodimer bands, denoted by asterisks, appear more prominently in the bottom panel. Thus, under the same condition the homodimer emit predominantly in the visible region, which has been assigned in many previous studies to fluorescence from the tautomeric configuration. The bands denoted by dots (•) in the middle panel are assigned in earlier studies to a 2:1 7AI−water complex.[16,34] Due to structural constrains, tautomerization of this species is restrained and emits only UV fluorescence from the locally excited state.

The results presented here show clearly that under the jet expansion conditions, the 7AI···δVL complex is not converted to the tautomeric form if excited to lower energy regions of the S_1 electronic state and emits in the ultraviolet region from the locally excited state. Obviously, this behavior is drastically different compared to its photophysics in MCH solution and also the photophysics of jet-cooled $7AI_2$. Thus, the photophysics of the complex is sensitively medium dependent, which is not the case for the homodimer. Recently, we also studied the LIF spectroscopy of jet-cooled 7AI···formamide and 7AI···pyrrolidinone complexes.[35,23] However, in both cases, only UV fluorescence from the locally excited state was detected.

Medium Effect on Photophysics of the 7AI···δVL Complex. The analysis presented above reveals that in the gas phase the ESDPT tautomerization of the complex is an energetically favored process. In MCH solution, because of the very small value of the dielectric constant (ε = 2.07) of the medium, neither of the two tautomeric forms of the complex gain any preferential stability, and the energy difference between the two tautomeric forms must be very similar to that in the gas phase. Therefore, the ESDPT tautomerization of the complex observed under this condition must be because of intrinsic stability of the tautomeric form and not induced in anyway by the hydrocarbon solvent, and the same argument also holds for the homodimer. Nevertheless, as detailed above, under the jet-cooling condition the ESDPT of the complex is fully blocked, and this can be rationalized only if the associated energy barrier is high. The FE spectra presented in Figure 5 shows that all the prominent bands are clustered near the $S_1 \leftarrow S_0$ origin only; i.e., the discrete vibronic bands are visible only up to ∼170 cm^{-1}, and beyond this the spectrum does not reveal any band corresponding to the complex. Furthermore, excitations of each of these bands result only UV fluorescence from the locally excited state of the complex. This behavior implies that the intrinsic ESDPT barrier must be larger than 170 cm^{-1} (∼2 kJ/mol), i.e., of the order of thermal energy at room temperature. On the other hand, as mentioned before, under the same condition the homodimer of the molecule emits only green tautomer fluorescence upon excitation to the S_1 zero-point level. Below, we argue first as to how this difference in tautomerization barrier of the two systems could arise.

An extensive theoretical study correlating the tautomerization barrier with the sequence of two proton transfers in the homodimer has been performed recently by Yu et al.[27] The study suggests that an asynchronous concerted transfer is the energetically favored pathway, and the associated energy barrier for calculation at CASPT2 level is only 0.5 kcal/mol. In contrast, the barrier for stepwise transfer is high, and in this case an intermediate charge transfer (CT) state is predicted, which is 4.9 kcal/mol lower in energy than the excited normal tautomeric form of the dimer. The barrier between this CT and final tautomeric configuration is ∼12 kcal/mol. Now, for the present 7AI···δVL complex, the hydrogen bond length and other attributes of the two linkages being considerably different, the details of the double proton transfer dynamics must be different from those of the homodimer. The most obvious effect of such differences could be on the sequences of the two protons exchange. The optimized geometric parameters of the complex shown in Figure 1 indicate that the N−H···O═C hydrogen bond length is significantly shorter compared to the other one, but in the case of the homodimer, the two hydrogen bonds are identical. As a consequence of such a difference, the intrinsic preference in sequence for the two hydrogen atom exchange of the complex must be different from that of the homodimer. As the electronic excitation of the complex is localized only on the 7AI moiety and the excited molecule is a stronger acid, the N−H proton could be transferred first to the carbonyl oxygen of the amide. Therefore, if the correlation between the sequence of proton transfers and energy barrier discussed above for the homodimer becomes also valid for the 7AI···δVL complex, the tautomerization barrier of the latter ought to be larger than that of homodimer.

Now, we discuss a few cases where the barrier crossing photophysical events are hindered under a jet expansion condition but occur in hydrocarbon solutions. A common optical process where barrier crossing is frequently encountered is the photoinduced CT process, either in molecular complexes consisting of donor−acceptor (D−A) molecular pairs or in a bichromophoric molecule where the D−A pairs are separated by some inert chain-like spacers.[36,37] The barrier originates primarily due to geometric constraints. For stability of the CT states, either due to Coulombic interaction or due to orbital overlap, the geometry needs to be reorganized. Under an isolated condition one can estimate the magnitude of the barrier by monitoring the onset of the CT when electronic excitations are performed with excess vibrational energies. For example, in the case of the bichromophoric anthracene−$(CH_2)_3$−dimethylaniline [A−(CH_3)−DMA] molecule,[36] although an extended trans−trans conformation is preferred in the ground state, for stability of the CT configuration the geometry needs to be reorganized to a folded form (gauche−gauche) in the excited state. The reorganization involves

dx.doi.org/10.1021/jp306959w | J. Phys. Chem. A 2012, 116, 9888−9896

internal rotations about several of its C−C bonds, and the associated energy barrier is ∼1200 cm^{-1} (∼3.5 kcal/mol). Nevertheless, in hexane solution at room temperature, the CT emission is the major component in the fluorescence spectrum of the molecule when excited near the S_1 electronic origin. Ultrafast time-resolved study reveals that only structured fluorescence bands of anthracene chromophore are observed in early segment of the decay period, but the broad CT fluorescence develops only after a waiting period ∼1.6 ns, which was associated with the conformational rearrangement time. In contrast, the jet-cooled molecule emits only UV fluorescence when excited near the $S_1 \leftarrow S_0$ origin level, but the onset of the CT emission is observed when the anthracene chromophore is excited with ∼900 cm^{-1} (2.6 kcal/mol) of excess vibrational energy. The results clearly demonstrate that the thermal energy available to different low-frequency chain modes of the molecule in hydrocarbon solution at room temperature helps crossing the said energy barrier. For the present 7AI···δVL complex, if the magnitude of effective barrier for stepwise ESDPT process is considered to be somewhat similar to that estimated for the homodimer, the tautomeric conversion is not expected to take place in a cold supersonic jet expansion environment. On the other hand, in a hydrocarbon solution at room temperature, the available thermal energy in various low-frequency modes help surmounting the ESDPT barrier as it happens in the case of crossing the CT barrier of A−(CH_3)−DMA molecule in hexane solution.

Excess vibronic energies are also required for triggering off CT processes in many of the 1:1 jet-cooled van der Waals complexes of donor−acceptor molecules. For example, we have shown recently that the jet-cooled homodimer of 2-methoxynaphthalene does not emit excimer fluorescence when excited to the S_1 origin (0_0^0) level, but this emission appears upon excitation of the low-frequency intermolecular vibrational modes.[37] The intrinsic barrier of the present 1:1 complex must be larger than 170 cm^{-1}. However, the system does not allow us to investigate directly the vibronic energy dependent photophysics because no discrete band is discernible in the FE spectrum of the complex beyond 170 cm^{-1} of the $S_1 \leftarrow S_0$ electronic origin. To overcome this limitation, we suggest adopting a more sophisticated double resonance scheme, i.e., prior to electronic excitation the complex can be vibrationally excited with respect to its intense $\nu_{C=O}$ or ν_{N-H} stretching modes. It is worth mentioning also that measurement of the intrinsic ESDPT barrier of the complex is not possible by measuring the temperature-dependent photophysics of the complex in a hydrocarbon solution, as typically done for estimating the reaction barriers in the solution phase. We have noted that in the MCH solution the ESDPT barrier of the complex is manifested when the temperature is lowered below −40 °C, and at this temperature the complex starts emitting dual fluorescence, of which the UV fluorescence (λ_{max} ∼ 350 nm) component is emitted from the locally excited state. However, there has been extensive discussion in the literature suggesting that this barrier originates due to increased viscosity of the medium at lowered temperatures, and not due to intrinsic ESDPT barrier of the dimer.[38] Very recently we have measured the photophysics of the doubly hydrogen bonded dimer of 7AI by isolating in cold inert gas matrixes, and it has been observed that ESDPT tautomerization is hindered almost fully under this condition.[39]

The other important factor that in principle can promote the ESDPT process of $7AI_2$ is the exciton interaction between the two identical moieties in the excited state. This interaction is completely absent in the present complex. However, it is worth mentioning that in a recent study it has been proposed that exciton interaction at the lowest excited (S_1) state of $7AI_2$ is very small, and the dimer has been suggested to be a weak coupling case in exciton theory.[7,12] The ESDPT tautomerization has been found to occur also in an isolated mixed dimer between 7AI and methyl substituted 7AI (Me-7AI) under the jet-cooling condition.[7] Thus, it was proposed in ref 7 that exciton interaction is not a significant factor for occurrence of ESDPT tautomerization. However, it is notable that in contrast to the present complex, the chromophoric parts of both moieties of the previously studied mixed dimer (Me-7AI···7AI) are same. Therefore, the role of a very subtle excitonic type interaction between two moieties with similar electronic structures on lowering ESDPT tautomerization barriers of 7AI containing systems under isolated conditions cannot be completely ruled out, and we believe this factor needs to be investigated further. A high-level electronic structure calculation is also essential to investigate the nature of ESDPT potential energy surface. We hope experimental finding presented in this report would prompt further studies in this direction.

Vibrational Analysis of the FE Spectrum of the 7AI···δVL Complex. The FE spectrum shown in Figure 5 (upper panel) displays pronounced activity for a large number of low-frequency vibrational modes. The displacements of these bands (cm^{-1}) with respect to the 0_0^0 transition frequency are much smaller compared to that of the lowest frequency vibronic band of the 7AI monomer (233 cm^{-1}) observed in its $S_1 \leftarrow S_0$ FE spectrum.[3] The low-frequency features in the upper trace of Figure 5 could be due to excitations of the following three types of vibrational modes of the complex. The major numbers of bands are for excitations of the six intermolecular vibrational modes, and the internal coordinates corresponding to these modes are the different geometric parameters of the doubly hydrogen-bonded interface of the complex. The other two types of low-frequency modes are out-of-plane distortion of 7AI ring and the ring puckering of δVL moiety. In the $\pi\pi^*$ excited state of the complex, where only the 7AI moiety is excited, the geometry of the δVL moiety remains practically unaffected (Table 3) and, according to our analysis (presented below), no vibrational transition, for which the mode belonging

Table 3. Predicted Changes in Geometric Parameters at the Hydrogen-Bonded Interface of the 7AI···δVL Complex Owing to $S_1 \leftarrow S_0$ Electronic Excitation[a]

geometric parameters	ground electronic state	locally excited state
N_{24}−H_{16} (Å)	2.20	2.11
H_{26}−O_6 (Å)	1.94	1.85
N_{24}−C_{23} (Å)	1.32	1.39
N_{24}−C_{25} (Å)	1.32	1.30
N_{17}−C_{25} (Å)	1.36	1.39
N_7−C_1 (Å)	1.34	1.335
C_1−O_6 (Å)	1.21	1.22
N_7−H_{16} (Å)	1.005	1.01
∠N_7−H_{16}−N_{24} (deg)	179.5	178.6
∠N_{17}−H_{26}−N_6 (deg)	171.1	172.7
∠N_{17}−C_{25}−N_{24} (deg)	125.7	124.3

[a]HF and CIS methods have been used with 6-31G* basis set to optimize the geometries in S_0 and S_1 states. The atom numbering is shown in Figure 1.

exclusively to either of these moieties appears in the lower energy region of the FE spectrum.

In Table 2 the frequencies of the observed vibronic bands and their tentative assignments are presented. To suggest these assignments, we have considered the ground and excited state frequencies of the modes of the complex predicted by electronic structure calculation, and a somewhat general behavior that frequencies of some of the intermolecular modes, e.g., intermolecular stretching vibration, are increased in the excited state. This happens because the hydrogen bonds in the excited state are stronger owing to enhanced acid−base character of the molecule, and this is consistent with the geometrical parameters of the hydrogen bonds predicted in the two electronic states (Table 3). The lowest frequency band at 22.5 cm^{-1} could be assigned to the fundamental of butterfly mode at the hydrogen bonded interface, and the corresponding calculated frequency is 23 cm^{-1}. A very short progression with respect to this mode is also visible in the spectrum and the band at 45 cm^{-1} can be assigned to overtone of this mode. Near this frequency, the fundamental of the out-of-plane twisting mode (Q_2) is also expected, but the spectrum does not show a distinct signature for this transition. The bands at 69 and 76 cm^{-1} are assigned to the fundamentals of in-plane and out-of-plane rocking of the two moieties (Q_3 and Q_4), respectively. The observed frequencies for these two transitions show excellent match with the calculated frequencies. The combination tones of these two modes with Q_1, i.e., ($Q_1 + Q_3$) and ($Q_1 + Q_4$) appear at 92 and 99 cm^{-1}, respectively. The next two prominent bands at 114.5 and 149 cm^{-1} are assigned to the fundamentals of the in-plane sliding (Q_5) and stretching (Q_6) modes, respectively. For both the modes, the excited state frequencies are expected to be larger compared to the ground state frequencies. Consistent with such expectations, the CIS calculation predicts the values of S_1 frequencies of these two modes ∼11% larger compared to the values in S_0 state, although the absolute values of the calculated frequencies are somewhat smaller than the observed values. On the other hand, the calculated frequencies by B3LYP method for these two modes in S_0 are 92 and 129 cm^{-1}, respectively. These predictions are usually considered to be more reliable compared to those by HF method. Now, if we consider that the frequencies in the excited state are about 10% larger compared to the corresponding ground state values, then the estimates match nicely with measured values. The remaining bands of the complex at 137, 145, 153, and 171 cm^{-1} can easily be assigned as combinations/overtones of the observed intermolecular fundamentals.

SUMMARY AND OUTLOOK

In this paper, we have shown that the ESDPT dynamics leading to tautomerization of a 1:1 complex between 7AI and δVL is efficient in hydrocarbon solution but hindered completely in a cold supersonic jet expansion. An energy balance analysis concerning the relative stability of the normal and tautomeric forms reveals that similar to the homodimer the ESDPT tautomerization of the complex is an energetically favorable process. The $S_1 \leftarrow S_0$ electronic transition energy (32 054 cm^{-1}) of the complex in the gas phase being similar to that of the homodimer, we propose a doubly hydrogen bonded cyclic structure for the complex, and this suggestion is consistent with the predictions of electronic structure calculation. The nonoccurrence of ESDPT of the complex under the jet-cooling condition has been interpreted in terms of a larger activation barrier with respect to that of homodimer. We suggest that the asymmetry of the two hydrogen bonds, which favors a sequential double proton exchange dynamics, could be the origin for the higher ESDPT barrier. Because of very weak intensities of the higher frequency vibronic bands in the $S_1 \leftarrow S_0$ absorption spectrum, we could not measure directly the tautomerization threshold of the complex under the jet-cooling condition. Measurement of the barrier is extremely important to reveal the correlation between the ESDPT barrier and proton transfer sequence. A high-level theoretical calculation is also essential to accurately map the double proton exchange potential energy surface of the complex in the exited state for more quantitative interpretation about origin of the barrier.

AUTHOR INFORMATION

Corresponding Author

*Phone: +91 33 2473 4971 (Ext. 1470). Fax: +91 33 2473 2805. E-mail: pctc@iacs.res.in.

Notes

The authors declare no competing financial interest.

ACKNOWLEDGMENTS

The authors sincerely acknowledge the financial support received from CSIR and Ramanna Fellowship grant of DST, Govt. of India, to carry out the research presented here. S K thanks CSIR for being awarded with a Senior Research Fellowship. The technical assistances provided by Nishir Roy, Jhankar Ghosh, Prabir Mandal and Joydeb Mandal are gratefully acknowledged.

REFERENCES

(1) Taylor, C. A.; El-Bayoumi, M. A.; Kasha, M. *Proc. Natl. Acad. Sci. U. S. A.* **1969**, *63*, 253−260.
(2) Ingham, K. C.; El-Bayoumi, M. A. *J. Am. Chem. Soc.* **1974**, *96*, 1674−1682.
(3) Fuke, K.; Yoshiuchi, H.; Kaya, K. *J. Phys. Chem.* **1984**, *88*, 5840−5844.
(4) Kim, S. K.; Bernstein, E. R. *J. Phys. Chem.* **1990**, *94*, 3531−3539.
(5) Douhal, A.; Kim, S. K.; Zewail, A. H. *Nature* **1995**, *378*, 260−263.
(6) Catalán, J. *Phys. Chem. Chem. Phys.* **2004**, *6*, 4467−4472.
(7) Komoto, Y.; Sakota, K.; Sekiya, H. *Chem. Phys. Lett.* **2005**, *406*, 15−19.
(8) Sakota, K.; Sekiya, H. *J. Phys. Chem. A* **2005**, *109*, 2722−2727.
(9) Kang, C.; Yi, J. T.; Pratt, D. W. *Chem. Phys. Lett.* **2006**, *423*, 7−12.
(10) Takeuchi, S.; Tahara, T. *Proc. Natl. Acad. Sci. U. S. A.* **2007**, *104*, 5285−5290.
(11) Kwon, O.-H.; Zewail, A. H. *Proc. Natl. Acad. Sci. U. S. A.* **2007**, *104*, 8703−8708.
(12) Sekiya, H.; Sakota, K. *J. Photochem. Photobiol. C: Photochem. Rev.* **2008**, *9*, 81−91 and references therein.
(13) Kwon, O.-H.; Lee, Y.-S.; Park, H. J.; Kim, Y.; Jang, D.-J. *Angew. Chem., Int. Ed.* **2004**, *43*, 5792−5796 and references therein.
(14) Kageura, Y.; Sakota, K.; Sekiya, H. *J. Phys. Chem. A* **2009**, *113*, 6880−6885.
(15) Chou, P.-T.; Martinez, M. L.; Cooper, W. C.; McMorrow, D.; Collins, S. T.; Kasha, M. *J. Phys. Chem.* **1992**, *96*, 5203−5205 and references therein.
(16) Yokoyama, H.; Watanabe, H.; Omi, T.; Ishiuchi, S.; Fujii, M. *J. Phys. Chem. A* **2001**, *105*, 9366−9374.
(17) Sakota, K.; Jouvet, C.; Dedonder, C.; Fujii, M.; Sekiya, H. *J. Phys. Chem. A* **2010**, *114*, 11161−11166.
(18) Chang, C.-P.; Wen-Chi, H.; Meng-Shin, K.; Chou, P.-T.; Clements, J. H. *J. Phys. Chem.* **1994**, *98*, 8801−8805.

(19) Chou, P.-T.; Wei, C.-Y.; Chang, C.-P.; Meng-Shin, K. *J. Phys. Chem.* **1995**, *99*, 11994−12000.
(20) Crespo-Hernández, C. E.; Cohen, B.; Hare, P. M.; Kohler, B. *Chem. Rev.* **2004**, *104*, 1977−2019.
(21) Löwdin, P. D. *Adv. Quantum Chem.* **1965**, *2*, 213−360.
(22) Chou, P.-T.; Wei, C.-Y.; Chang, C.-P.; Chiu, C.-H. *J. Am. Chem. Soc.* **1995**, *117*, 7259−7260.
(23) Mukherjee, M.; Karmakar, S.; Chakraborty, T. *Chem. Phys. Lett.* **2012**, *519*, 34−39.
(24) Boys, S. F.; Bernardi, F. *Mol. Phys.* **1970**, *19*, 553−566.
(25) Frisch, M. J.; Trucks, G. W.; Schlegel, H. B.; Scuseria, G. E.; Robb, M. A.; Cheeseman, J. R.; Montgomery, J. A., Jr.; Vreven, T.; Kudin, K. N.; Burant, J. C.; et al. *Gaussian 03*, Revision E.01; Gaussian, Inc.: Wallingford, CT, 2004.
(26) Ishikawa, H.; Yabuguchi, H.; Yamada, Y.; Fujihara, A.; Fuke, K. *J. Phys. Chem. A* **2010**, *114*, 3199−3206.
(27) Yu, X.-f.; Yamazaki, S.; Taketsugu, T. *J. Chem. Theory Comput.* **2011**, *7*, 1006−1015 and references therein.
(28) Ando, K.; Hayashi, S.; Kato, S. *Phys. Chem. Chem. Phys.* **2011**, *13*, 11118−11127.
(29) Serrano-Andrés, L.; Merchán, M. *Chem. Phys. Lett.* **2006**, *418*, 569−575.
(30) Catalán, J.; Pérez, P.; dell Valle, J. C.; de Paz, J. L. G.; Kasha, M. *Proc. Natl. Acad. Sci. U. S. A.* **2004**, *101*, 419−422.
(31) Moreno, M.; Douhal, A.; Guallar, V.; Lluch, J. M.; Castono, O.; Frutos, L. M. *J. Phys. Chem. A* **2001**, *105*, 3887−3893.
(32) Catalán, J.; dell Valle, J. C.; Kasha, M. *Proc. Natl. Acad. Sci. U. S. A.* **1999**, *96*, 8338−8343.
(33) Douhal, A.; Guallar, V.; Moreno, M.; Lluch, J. M. *Chem. Phys. Lett.* **1996**, *256*, 370−376.
(34) Hazra, M. K.; Mukherjee, M.; Ramanathan, V.; Chakraborty, T. *J. Chem. Sci.* **2012**, *124*, 131−139.
(35) Hazra, M. K.; Mukherjee, M.; Goswami, D.; Chakraborty, T. *Chem. Phys. Lett.* **2011**, *503*, 203−209.
(36) Syage, J. A.; Felker, P. M.; Zewail, A. H. *J. Chem. Phys.* **1984**, *81*, 2233−2256.
(37) Das, A.; Mahato, K. K.; Chakraborty, T. *J. Chem. Phys.* **2001**, *114*, 8310−8315.
(38) Catalán, J. *J. Phys. Chem. A* **2010**, *114*, 5666−5673.
(39) Mukherjee, M.; Bandyopadhyay, B.; Chakraborty, T. *Chem. Phys. Lett.* **2012**, DOI: http://dx.doi.org/10.1016/j.cplett.2012.07.045.